RESEARCH PAPER

Fabrication of Macro- and Micropore Forming DCPD/β-TCP Porous Scaffolds: Effect of Setting-Time Reaction and Acidic Calcium Phosphate Solution

Ahmed Hafedh Mohammed Mohammed[1,2], Khairul Anuar Shariff[1,*], Mohamad Hafizi Abu Bakar[3], Hasmaliza Mohamad[1]

* *biokhairul@usm.my*

[1] School of Materials and Mineral Resources Engineering, Engineering Campus, Universiti Sains Malaysia, 14300, Nibong Tebal, Penang, Malaysia

[2] Department of Materials Engineering, College of Engineering, Mustansiriyah University, Baghdad, Iraq

[3] Bioprocess Technology Division, School of Industrial Technology, Universiti Sains Malaysia, 11800, Gelugor, Penang, Malaysia

Abstract: *The coated β-tricalcium phosphate (β-TCP) with dicalcium phosphate dihydrate (DCPD) has attracted much attention in the biomaterials field due to the increase in its osteoconductivity. Besides, the porous bioceramic scaffolds with controlled pore sizes are significant in stimulating bone-like cell activity. In this study, the effect of the setting-time process and acidic-calcium phosphate (CaP) concentrations on the fabrication and properties of porous DCPD/β-TCP scaffolds were studied. Subsequently, the specimens were examined using X-ray Diffraction (XRD), scanning electron microscope (SEM), compression strength and Fourier Transforms Infrared (FTIR). The study results revealed that the porous DCPD/β-TCP scaffolds with macro- and micropore sizes were successfully obtained after the 300-600 μm of porous β-TCP granules were exposed to an acidic-CaP solution. Furthermore, the setting-time process and acidic-CaP concentrations increased the DCPD interlocking between granules, and the mechanical strengths of scaffolds increased up to 0.5 MPa. Meanwhile, the porosity levels were changed based on the formation of DCPD crystals. This study was expected to provide novel insights to researchers in the field of bioceramics through its investigation of the creation of porous DCPD/β-TCP scaffolds.*

Keywords: *Bioceramic, Ceramic coating, Calcium phosphate, Bone remodelling, Porous β-TCP scaffolds.*

1. INTRODUCTION

Porous calcium phosphate (CaP) scaffolds are commonly employed in oral surgery to help repair damaged bone due to its biological properties [1–4]. Among the numerous CaP groups, beta-tricalcium phosphate (β-TCP) has shown good bone cell growth. This is because of its good bioresorbability and osteoconductivity in small bone defect locations [5–8]. However, the osteoconductivity of these types of materials is still low in large bone defect areas. Therefore, recent studies found that the appropriate dicalcium phosphate dihydrate (DCPD [$CaHPO_4.2H_2O$]) amounts coated on the β-TCP granules significantly improved bone osteoconductivity [9, 10]. Notably, in physiological conditions in the human body, DCPD has the highest solubility value when compared to other calcium phosphate groups [11]. Consequently, the DCPD coating technique may offer an alternative approach for enhancing the creation of bone bridges between host bone surfaces and bone substitutes [11]. Besides, bone-like cell activity is strongly influenced by the type of bioceramic coating material, pore sizes and interconnective porosity. Bioceramic scaffolds can be degraded quickly due to micro- and macropores, which regulate cell adhesion, proliferation, and differentiation [2, 11–15].

Moreover, numerous studies have been conducted to fabricate macropore granular cement by interlocking the β-TCP granules with DCPD crystals. For example, Khairul et al. and Pham et al. fabricated macropore granule cement of α-TCP by exposing dense granules to acidic-calcium phosphate (CaP) solutions [16, 17]. They found that the DCPD crystals interlocked between granules and created macropore structures. However, the porosity levels of these granule cements were lower than 50%. Furthermore, Haifaa et al. discovered that the setting time process influences the DCPD formations precipitated between β-TCP foam granular cement [18]. Meanwhile, a previous study done by Khairul et al. reported that the DCPD crystals

can be regulated by changing the acidic CaP concentrations [19]. However, no studies conducted to evaluate the setting of porous β-TCP granules to form the macro- and microporous structure of DCPD/β-TCP scaffolds by bridging the DCPD crystals between porous granules. Also, no study has been made to establish the impact of the setting-time process and acidic CaP concentrations on the precipitation of DCPD crystals on and between the porous β-TCP granules to produce macro- and microporous β-TCP/DCPD scaffold. Therefore, this study aimed to set the porous β-TCP granules to form macro- and microporous DCPD/β-TCP scaffolds after being exposed to the acidic-CaP solution using different setting-time reactions and acidic-CaP concentrations. The study results will give a new understanding regarding the effect of the setting-time reaction and acidic-CaP concentrations on the formation of DCPD crystals to produce the porous DCPD/β-TCP scaffolds. Consequently, this new porous scaffold will help increase healing in the large bone defect area.

2. EXPERIMENTAL PROCEDURES

2.1. Porous β-TCP Granules Fabrication

The dry powder of DCPD [($CaHPO_4.2H_2O$) Wako] and calcium carbonate powders [(calcite: $CaCO_3$) Wako] were obtained after being mixed with an ethanol solution using a planetary milling machine (Pulverisette 5, Germany) running at 200 rpm for 6 h. Then, it was dried at 60°C for 6 h. The slurry powder produced was turned into a finely ground powder [9]. Notably, if DCPD contains a calcium salt and the total Ca/P molar ratio is 1.5, DCPD and the calcium compound may convert into β-TCP after sintering [20]. Furthermore, the sodium chloride (NaCl) powders were mixed with the fine powders at the weight ratios of 40:60, respectively. NaCl powders were frequently utilized to create different micropore diameters depending on the composition's weight ratio [21]. Then, the powders were combined within a rotary container

for a duration of 2 h using a milling machine, then were compacted using an oil press machine at 50 MPa and heated in a furnace at a temperature of 1100ºC to help create pores inside β-TCP structures. A common technique for creating porous structures is by introducing a porogen. Finally, the compressed pellets followed crushing and sieving processes, which produced granular sizes between 300 μm to 600 μm of porous β-TCP granules.

2.2. Synthesis of an Acidic Calcium Phosphate Solution

An acidic-CaP solution employed in the current study was synthesised from monocalcium phosphate monohydrate (MCPM), [$Ca(H_2PO_4)_2 \cdot H_2O$ (Sigma-Aldrich, USA)] and diluted phosphoric acids (H_3PO_4) (Merck, USA) solution. Besides, the concentrations of acidic-CaP solutions utilised in the study are presented in Table 1 [19].

2.3. Scaffold Fabrication via Dissolution-Precipitation Reaction

The creation of porous DCPD/β-TCP scaffolds was produced using a setting reaction occurring during the dissolution precipitation process. In this setting reaction process, after the acidic-CaP solution was added to the mould containing the porous β-TCP granules, it will interact to supply Ca^{2+} and PO_4^{3-} to the solution and when reaches its supersaturation level due to the continuous dissolution of Ca^{2+} and PO_4^{3-} from the β-TCP granules, DCPD crystals precipitate on the surfaces and inside the porous structure of β-TCP granules during the precipitation-dissolution reactions [20]. Furthermore, in this experiment, the different setting-time reactions at (2, 4, 6, and 8 h) and three various concentrations of acidic-CaP solution, as shown in Table 1, were employed. Notably, to precisely characterize the modifications in scaffold properties that occur throughout the fabrication process, the time points for the setting-time reactions were selected using systematic techniques.

Table 1. Ca^{2+} and PO_4^{3-} concentrations in the acidic-CaP solutions.

Concentration mmol/l		Concentration mmol/l	
H_3PO_4	MCPM	Ca^{2+}	PO_4^{3-}
25	50	50	75
25	75	75	100
25	100	100	125

These particular periods were chosen to provide an in-depth comprehension of the scaffolds' development and stabilization processes across time. In this reaction process, the porous β-TCP granules were added into a stainless-steel mould divided into two parts. The dimensions were 6 mm in diameter and 3 mm in height. Subsequently, the granules had been exposed to an acidic-CaP solution at a temperature of 25ºC. The acidic volume to granular mass ratio was maintained at 0.3 ml to 0.2 g. Finally, the porous scaffolds designed were soaked in acetone to arrest the process [16].

2.4. Scanning Electron Microscopy (SEM)

The fabricated porous DCPD/β-TCP scaffolds were coated with gold-palladium for 2 min. Then, were used to examine the morphology through an SEM (S-3400N; Hitachi High Technologies Co., Tokyo, Japan) at a 15 kV acceleration voltage. SEM measured the macro- and microporosity of DCPD/β-TCP scaffolds using PoroMetric.

2.5. X-ray Diffraction Analysis

All set and unset scaffolds were crushed to powder and carried out using an X-ray diffractometer (Bruker Analytical X-ray Systems); 40 kV and 40 mA were used. The diffraction angles were scanned from 10° to 40° at 2Θ, scanning step 2°/min. Meanwhile, the phases have been identified using a JCPDS card (Joint Committee on Powder Diffraction Standards). MDI Jade 5.0 Software (Materials Data Inc., USA) was also used to compute DCPD concentrations between β-TCP granules [19].

2.6. Porosity Analysis

The numerous porous scaffolds' porosity was calculated using liquid displacement. The porous DCPD/β-TCP scaffold's dry weight was subjected to a 48-h immersion in ethanol. The following equation estimated the porous scaffolds' 48-h ethanol absorption [22, 23].

$$P(\%)= (W_2-W_1)/(^D ethanol+^V scaffold)\times 100 \quad (1)$$

W_2 and W_1 represent the wet and dry weights of scaffolds, respectively. Vscaffold is the volume of the wet scaffold, and Dethanol stands for the ethanol density at room temperature.

2.7. Compression Strength

The measurements of compressive strength were employed to evaluate the porous scaffolds designed. These porous DCPD/β-TCP scaffolds were tested under ASTM-D-695-96 using an Instron 3369 at 1.0 mm/min test speed and 5 kN cell load. Five samples were given for each test.

2.8. Functional Group Analysis

Fourier transforms infrared (FTIR; Perkin Elmer, Spectrum One, USA) was used to analyse the present bonding. The specimens were combined in a 1:10 ratio with potassium bromide (KBr; Sigma Aldrich, USA) after being crushed into a smooth powder in an agate mortar [24]. The FTIR spectrum exhibits a wavelength resolution of 4 cm^{-1} across the frequency range from 4000 to 400 cm^{-1}.

2.9. Statistical

The average standard deviation was used in this study to present the quantitative data. One-way ANOVA was used to evaluate the statistical analyses using the following thresholds: *$p< 0.05$, **$p< 0.01$, ***$p< 0.001$ and n.s= insignificant. Additionally, the statistical analysis compared the variations in DCPD quantities, compressive strength, and porosity levels of all produced porous DCPD/ β-TCP scaffolds.

3. RESULTS AND DISCUSSION

3.1. Setting-Time Reactions

3.1.1. *Surface morphologies and appearance views*

Fig. 1 displays SEM images and the appearance of porous DCPD/β-TCP scaffolds produced with varied reaction times (2, 4, 6, and 8 h). These porous scaffolds were fabricated through the immersion of porous β-TCP granules, with a size range of 300-600 μm, in an acidic-CaP solution containing 50 mmol/l MCPM and 25 mmol/l H_3PO_4 at (50 mmol/l). The study showed that porous DCPD/ β-TCP scaffolds with micro- and macropores have been produced. The appearance view in Fig. 1 (a, d, g, and j) demonstrated that the setting-time reaction only noticed the set scaffolds at 6 and 8 h.

This suggests that dissolution-precipitation processes affected the set of scaffolds. Morphologically, setting-time reaction affected plate-like crystal (DCPD) precipitation between porous granules. As shown in Fig. 1 (b, e, h, and k) and (c, f, i, and l), SEM images at low and high magnifications showed plate-like crystals (DCPD) interlocked between granules and

increased with setting-time reactions, which showed set porous DCPD/β-TCP scaffolds successfully produced with larger DCPD crystals.

3.1.2. *Phase analyses*

Fig. 2 depicts the XRD peaks of set and unset porous DCPD/β-TCP scaffolds that were fabricated by exposing porous β-TCP granules to 50 mmol/l of acidic-CaP solution at four different setting-time reactions (2, 4, 6, and 8 h) were performed. Notably, the porous β-TCP granules and purchased DCPD were used for

comparison. The findings demonstrated that at 2θ= 11.78º, a new peak related to DCPD was found at 2, 4, 6, and 8 h setting-time reactions, while at 2θ= 31.2, the peaks belonged to β-TCP and remained unchanged regardless of setting-time reactions [25].

These were aligned with SEM results and showed the DCPD crystals at 2, 4, 6, and 8 h setting times employed. This indicated that the XRD detected the DCPD formed between the granules, and the values of the peaks exhibited a rise as the setting time increased.
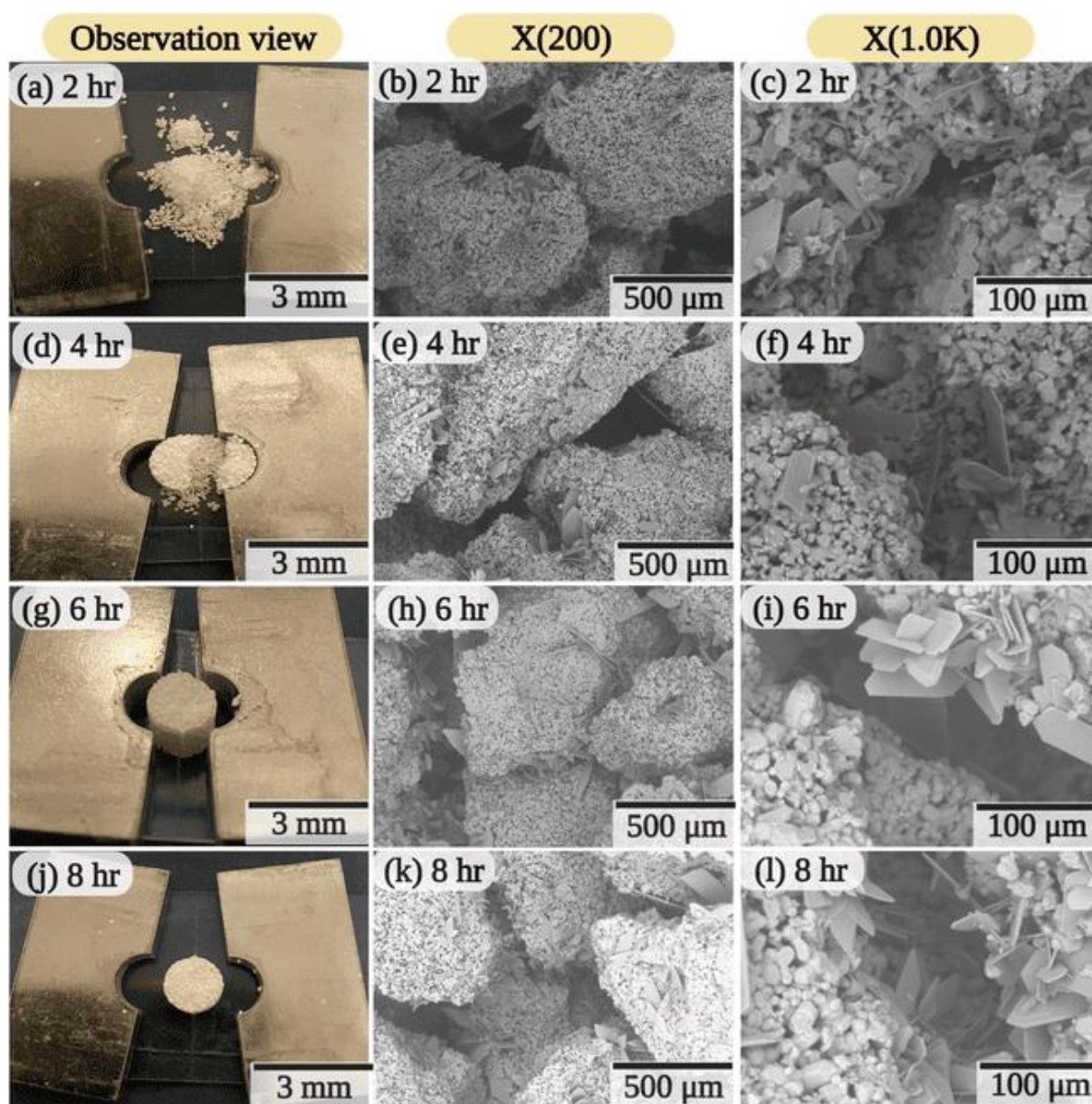

Fig. 1. SEM images and observation views of set and unset porous DCPD/β-TCP scaffolds fabricated using 300-600 μm granular sizes through different setting-time reactions at 2, 4, 6, and 8 hours. Note: the plate-like crystals bridged between the porous granules refer to DCPD crystals precipitated.
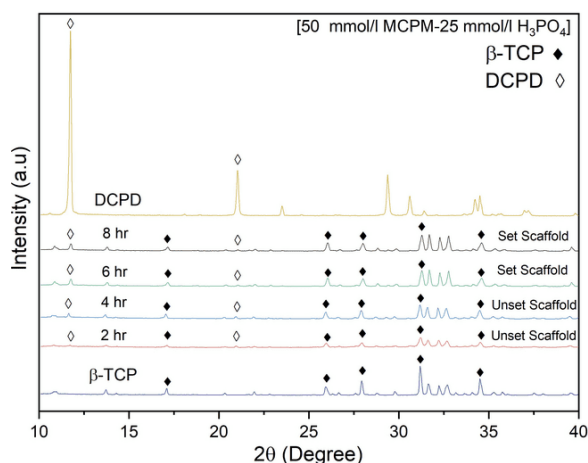
Fig. 2. The XRD peaks of unset and set porous DCPD/β-TCP scaffolds after exposure the 300-600 μm of porous β-TCP granules with 50 mmol/l concentrations of acidic-CaP solution at four different setting-time reactions [2, 4, 6, and 8 hours].

3.1.3. *Functional groups*

Fig. 3 displays FTIR results of unset and set porous DCPD/β-TCP scaffolds produced with varying setting times (2 h, 4 h, 6 h, and 8 h) using 50 mmol/L acidic-CaP concentrations. Specifically, β-TCP porous granules and purchased DCPD were employed as controls.
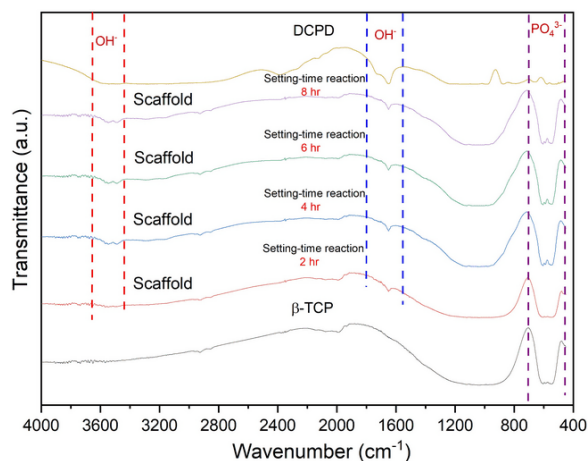

Fig. 3. The FTIR results of porous DCPD/β-TCP scaffolds after exposing 300-600 μm of porous β-TCP granules to 50 mmol/l of acidic-CaP solution at four different setting reaction times [2, 4, 6, and 8 hours].

The findings showed only PO_4^{3-} functional groups were revealed in the β-TCP at 550-600 cm^{-1} [26]. Besides, the OH$^-$ functional groups were detected after setting-time reactions of exposed porous granules of β-TCP with an acidic-CaP solution. These OH$^-$ chemical functional groups present in the set and unset

porous scaffolds were detected at wavenumbers of 1638 cm^{-1} and 3436 cm^{-1}, respectively. Which refers to DCPD inside the porous scaffolds fabricated [26].

The DCPD formations present in the fabricated porous DCPD/β-TCP scaffolds were compared to comprehend the properties of DCPD bridged with porous β-TCP granules. Therefore, these results were consistent with SEM images and XRD peaks obtained.

3.2. Acidic Calcium Phosphate Concentrations

3.2.1. *Surface morphologies*

Fig. 4 shows the SEM morphology of porous DCPD/ β-TCP scaffolds fabricated via dissolution precipitation reaction using three different acidic-CaP solutions. Based on the setting-time reactions as stated above, the set porous scaffold was fabricated using 50 mmol/l of the acidic-CaP at 6 and 8 h. Therefore, the selected time was based on setting-time reactions to assess the effect of different acidic-CaP concentrations 50 mmol/l, [75 mmol/l MCPM-25 mmol/l H$_3$PO$_4$] (75 mmol/l), and [100 mmol/l MCPM-25 mmol/l H$_3$PO$_4$] (100 mmol/l) on porous scaffold properties.

The findings obtained from using different acidic-CaP concentrations demonstrated that the plate-like crystals (DCPD) inside porous DCPD/β-TCP scaffolds increased with increasing acidic-CaP concentrations. Indicates that the precipitation of plate-like crystals (DCPD) between the porous granules influenced the set porous DCPD/β-TCP scaffolds. Furthermore, the slices of DCPD formation precipitated by using 100 mmol/l of an acidic-CaP solution were bigger than those of DCPD precipitated by using 50 mmol/l and 75 mmol/l. Indeed, this phenomenon might be attributed to the porous nature of the granules employed, as the dimensions of the pores significantly impact the dissolution precipitation reaction. The pore sizes and porosity notably provide high surface area [2]. Therefore, it is comprehensible that increasing the setting-time reactions and using an acidic-CaP solution stimulated higher DCPD formation between porous granules due to the high surface area provided by pore geometry. Moreover, the results of the current investigation clearly show that when porous granules were reacted with an acidic-CaP solution at room temperature, the interconnected porosity with the micro- and

macropore DCPD/β-TCP scaffold was successfully achieved. Besides, The DCPD crystals were interlocked between porous granules, which produced interconnected macropores.

3.2.2. *Phase analysis*

Fig. 5 shows the XRD results of set DCPD/β-TCP scaffolds fabricated after subjecting the porous β-TCP granules to three concentrations of an acidic-CaP solution. Furthermore, the findings revealed an increase in DCPD peaks when the concentration of an acidic-CaP solution increased.

Besides, as illustrated by Fig. 6, a more concentrated acidic-CaP solution can dissolve β-TCP granules and precipitate larger amounts of DCPD between porous β-TCP granules. The findings were consistent with SEM images presented in Figure 4, which depicted increased amounts of DCPD crystals as the concentrations of acidic CaP were increased.

Fig. 4. SEM images for 300-600 μm of porous DCPD/β-TCP scaffolds created by using different acidic-CaP concentrations at 8 hours. Note: the plate-like crystals bridged between the porous granules refer to DCPD crystals precipitated.

Fig. 5. The XRD patterns for 300-600 μm of porous DCPD/β-TCP scaffolds were fabricated with three concentrations.

Fig. 6. The amounts of DCPD formations in porous DCPD/β-TCP scaffolds fabricated by exposing 300-600 μm of porous β-TCP granules to three different concentrations of an acidic-CaP solution. (Note: *p< 0.05, and ***p< 0.001).

3.2.3. *Porosity analysis*

Fig. 7 shows the porosity of porous DCPD/β-TCP scaffolds manufactured using various concentrations of acidic CaP. The findings demonstrated that pore sizes inside the granules highly influenced the scaffold's porosity and precipitating DCPD formations, which showed a porosity level of around 70.3% after exposure to 50 mmol/l of acidic. In comparison, these porosities decreased to 68.1 % after exposed to 100 mmol/l. This is due to the DCPD formations that increased and infiltrated inside pore sizes with high acidic-CaP concentrations. Besides, the micro- and macropore sizes were successfully fabricated and changed based on the DCPD crystals precipitated between the porous granules. Consequently, the porosity levels were highly

related to the DCPD formed between and inside the porous granules.

Fig. 7. The porosity of porous DCPD/β-TCP scaffolds after exposing the 300-600 μm of porous β-TCP granules to three different concentrations of an acidic-CaP solution. (Note: *p< 0.05).

3.2.4. *Mechanical strength analysis*

Fig. 8 demonstrated the compression strength of set porous DCPD/β-TCP scaffolds created with three different concentrations of acidic-CaP solutions.
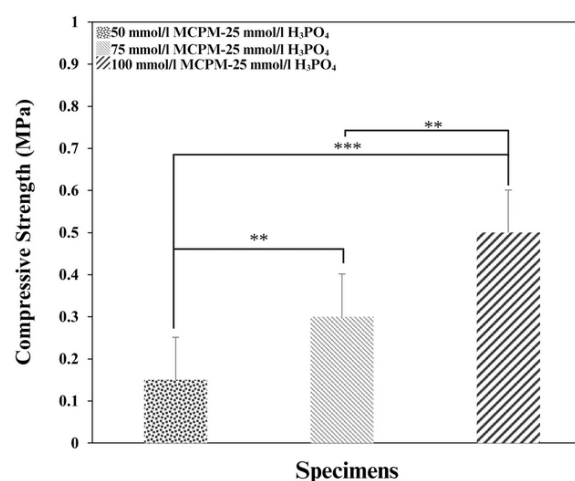

Fig. 8. The compression strength of porous DCPD/β-TCP scaffolds produced with three different concentrations of an acidic-CaP solution (Note: n.s= insignificant and **p< 0.01).

The obtained graph observed that when the acidic-CaP concentrations increased, the compression strength increased. This is due to the DCPD layers interlocked between and inside the porous granule. Furthermore, the compression strength of the set porous scaffold fabricated with acidic-CaP concentrations of 50, 75, and 100

mmol/l were 0.15 MPa, 0.3 MPa, and 0.5 MPa, respectively. These results revealed that the strength of the scaffold was controlled by the DCPD crystals that were interposed between the porous granules. Consequently, it is understood that the concentrations of an acidic-CaP solution were responsible for the increase in scaffolds' compressive strength due to the increased DCPD crystals precipitated.

3.2.5. *Functional groups*

Fig. 9 depicts the FTIR results of porous DCPD/β-TCP scaffolds produced using three different acidic-CaP concentrations. The chemical functional groups obtained, such as OH^- and PO_4^{3-}, were considered in this research. Likewise, only PO_4^{3-} functional groups were detected in β-TCP at 550-600 cm^{-1} [26]. The presence of OH^- functional groups was observed after the reaction between porous β-TCP granules and acidic-CaP solutions. Similarly, the above-mentioned functional groups were seen at wavenumbers of 1638 cm^{-1} and 3436 cm^{-1}, indicating the existence of DCPD within the scaffolds' compositions [26].

Fig. 9. The FTIR results for the 300-600 μm of porous DCPD/β-TCP scaffolds produced after the porous β-TCP granules were reacted with three different concentrations of an acidic-CaP solution.

4. CONCLUSIONS

The macro- and micropores of porous DCPD/β-TCP scaffolds have been successfully designed using a setting reaction process by exposing 300-600 μm of porous β-TCP granules to an acidic-CaP solution at different setting-time reactions and concentrations of acidic-CaP solutions. In the

setting-time process at 8 h and with high acidic-CaP concentration (100 mmol/l), the DCPD formations and mechanical strength of set DCPD/β-TCP porous scaffolds increased.

REFERENCES

[1]. Lett, J. A., M, S., and K, R., "Porous hydroxyapatite scaffolds for orthopedic and dental applications- the role of binders," Mater. Today, Proc., 2016, 3, 1672–1677.

[2]. Ahmed, H. M. M., Khairul, A. S., Dian, A. W., Mohamad, H. A. B., and Hasmaliza, M., "A comprehensive review of the effects of porosity and macro- and micropore formations in porous β-TCP scaffolds on cell responses." J Aust. Ceram. Soc., 2023, 1–15.

[3]. Foroutan, S., Hashemian, M., and Khandan, A. S., "A Novel Porous Graphene Scaffold Prepared Using Freeze-drying Technique for Orthopedic Approaches: Fabrication and Buckling Simulation Using GDQ Method." Iranian Journal of Materials Science and Engineering., 2020, 17, 62–76.

[4]. Farnaz, D. F., Ahmad, R. S., and Azadah, A., "Fabrication and Evaluation of in Vitro Studies of Biodegradable and Antibacterial Composite Scaffolds Based on Polylactic Acid-Polycaprolactone-Hydroxyapatite Reinforced with Graphene and Zinc Oxide Nanoparticles for Use in Orthopedic Surgery." Iranian Journal of Materials Science and Engineering., 2022, 19, 1–19.

[5]. Gangyuan, B., Lina, M., Sa, L., Xiupeng, Z., Junzhong, Y., Zhongrun, Y., Shenggui, C., and Li, R., "DLP printed β-tricalcium phosphate functionalised ceramic scaffolds promoted angiogenesis and osteogenesis in long bone defects." Ceram. Int., 2022, 48,

26274–26286.

[6]. Gerry, L. K., Mani, D., and Antonios, G. M., "Materials design for bone-tissue engineering." Nature Reviews Materials., 2020, 5, 584–603.

[7]. Eric, R., and Shuo, Y., "Compressive strength of β-TCP scaffolds fabricated via lithography-based manufacturing for bone tissue engineering." Ceram. Int., 2022, 48, 15516–15524.

[8]. Hang, Z., Hao, Z., Yinze, X., Lanlan, D., and Xiang, L., "Development of hierarchical porous bioceramic scaffolds with controlled micro/nano surface topography for accelerating bone regeneration." Materials Science and Engineering: C., 2021, 130, 112437.

[9]. Khairul, A. S., Kanji, T., and Kunio, I., "Fabrication of dicalcium phosphate dihydrate-coated β-TCP granules and evaluation of their osteoconductivity using experimental rats." Materials Science and Engineering C, 2017, 75, 1411–1419.

[10]. Nur, Z. M. Z., Ahmed, H. M. M., Mamun, K. S., Khairul, A. S., and Mohamad, H. A. B., "Behavioural responses of bone-like cells on dense and porous dicalcium phosphate dihydrate-coated β-tricalcium phosphate granules." J Aust. Ceram. Soc., 2023, 1–9.

[11]. Ahmed, H. M. M., Khairul, A. S., Mohamad, H. A. B., and Hasmaliza, M., "A review on the behavioral responses of osteoclast and osteoblast cells on the near-surface of the bioceramic coating: roles of ions released, solubility, and pH." J Aust. Ceram. Soc., 2022, 1–13.

[12]. Ke, Z., Yubo, F., Nicholas, D., and Xiaoming, L., "Effect of microporosity on scaffolds for bone tissue engineering." Regen Biomater., 2018, 5, 115–124.

[13]. W, B. S., Maiko, O., Zhen, Z., Hwa, K. N., Younghun, J., Gefei, W., Peter, X. M., Nan, E. H., and Yuji, M., "Macropore design of tissue engineering scaffolds regulates mesenchymal stem cell differentiation fate." Biomaterials., 2021, 272, 120769.

[14]. Sultana, N., Hassan, M. I., Ridzuan, N., Ibrahim, Z., and Soon, C. F., "Fabrication of Gelatin Scaffolds Using Thermally Induced Phase Separation Technique."

International Journal of Engineering., 2018, 31, 1302–1307.

[15]. Israa, K. S., and Batool, A. A. J., "Fabrication of Porous Biologic Hydroxyapatite Scaffold Reinforced with Polymer Coating for Bone Tissue Engineering Candidate." Iranian Journal of Materials Science and Engineering., 2023, 20, 1–10.

[16]. Khairul, A. S., Kanji, T., and Kunio, I., "Fabrication of interconnected pore forming α-tricalcium phosphate foam granules cement." J. Biomater Appl., 2016, 30, 838–845.

[17]. Pham, T. K., Kunio, I., Kanji, T., "Setting reaction of α-TCP spheres and an acidic calcium phosphate solution for the fabrication of fully interconnected macroporous calcium phosphate." Ceram. Int., 2015, 41, 13525–13531.

[18]. Haifaa, A. M. Z., Khairul, A. S., Mohamad, H. A. B., and Mohamad, N. A., "Effect of Different Granular Size on the Properties of Porous β-Tricalcium Phosphate Foam Granular Cements." Key Eng. Mater., 2020, 829, 23–27.

[19]. Khairul, A. S., Kanji, T., and Kunio, I., "Regulation of DCPD formation on β-TCP granular surface by exposing different concentrations of acidic calcium phosphate solution." Key Eng Mater., 2016, 696, 27–31.

[20]. Kunio, I., Tansza, S. P., Akira, T., Keisuke, T., and Kanji, T., "Fabrication of interconnected porous β-tricalcium phosphate (β-TCP) based on a setting reaction of β-TCP granules with HNO_3 followed by heat treatment." Journal of biomedical materials research. Part A., 2018, 106, 797-804.

[21]. Ruiz-Aguilar, C., Ulises, O., and Ismelí, A., "Novel β-TCP scaffold production using NaCl as a porogen for bone tissue applications." Ceram. Int., 2021, 47, 2244-2254.

[22]. Torres, A. L., Gaspar, V. M., Serra, I. R., Diogo, G. S., Fradique, R., Silva, A. P., and Correia, I. J., "Bioactive polymeric-ceramic hybrid 3D scaffold for application in bone tissue regeneration." Materials Science and Engineering C., 2013, 33, 4460–4469.

[23]. Serra, I. R., Fradique, R., Vallejo, M. C., Correia, T. R., Miguel, S. P., and Correia, I. J., "Production and characterisation of chitosan/gelatin/β-TCP scaffolds for improved bone tissue regeneration." Materials Science and Engineering: C., 2015, 55, 592–60.

[24]. Anna, Ś., Czesława, P., Marek, G., and Zofia, P., "The FTIR spectroscopy and QXRD studies of calcium phosphate based materials produced from the powder precursors with different CaP ratios." Ceram. Int., 1997, 23, 297–304.

[25]. Naoyuki, F., Kanji, T., Yoshihide, M., and Kunio, I., "Effect of citric acid on setting reaction and tissue response to β-TCP granular cement." Biomedical Materials., 2017, 12, 015027.

[26]. Lim, J. W., Khairul, A. S., Syed, A. M., Mohamad, H. A. B., and Arief, C., "Self-setting β-tricalcium phosphate granular cement at physiological body condition: effect of citric acid concentration as an inhibitor." J Aust. Ceram. Soc., 2021, 57, 687–696.